

IMAGE RECONSTRUCTION FROM TRUNCATED PROJECTIONS : A LINEAR PREDICTION APPROACH

N. Srinivasa* V. Krishnan^o K.R. Ramakrishnan* K. Rajgopal*

*Dept. of Elect. Engg., Indian Institute of Science, Bangalore, INDIA.

^oSchool of Automation, Indian Institute of Science, Bangalore, INDIA.

^oDept. of Elec. Engg., University of Lowell, Lowell, Mass., USA.

Abstract

Unambiguous reconstruction is not possible with truncated projections. In order to reduce the ambiguity in the reconstructed image, several authors have suggested that a simple 'completion' involving extrapolation of the truncated projection is sufficient. In this paper a method based on a Linear Prediction approach is proposed for obtaining the missing part in the projection. Reconstruction is then carried out using the Convolution Backprojection (CBP) method [1]. Simulation results showing the effectiveness of this method in extracting significantly more information from truncated projections are presented.

Introduction

Image reconstruction from projection relies on the fact that the object function is represented completely by a set of line integrals so that a knowledge of the projections is sufficient to unambiguously determine the structure of the object. In medical imaging, projections physically correspond to the linear attenuation of X-rays, the time-of-flight of an ultrasonic pulse or the total radio activity in an elemental volume of a distributed isotope. Other application areas where images are reconstructed from projections are Nuclear Magnetic Resonance, electron microscopy, radio astronomy, etc.,.

In practice, there are many situations wherein the available projection is truncated (also referred to as 'limited field of view' and 'restricted region scan') [2]. For instance, the projections are necessarily truncated if the object being examined has dimensions larger than the field of view of the imaging system, as in the case of Gamma cameras in nuclear medicine. In clinical situations where the diseased area is already localized from a previous study and a followup scan of the Region Of Interest (ROI) is required, a restricted region scan is done in order to minimize the radiation dosage. Here projection data is intentionally truncated as the external region is not subjected to radiation. In electron microscopy, it is known that in negatively stained preparations of certain biological objects, the overall distribution of stain does not preserve the symmetries of the object, especially the outer parts of the projections, thus resulting in truncated projections. In all these cases, reconstruction has

to be attempted with the available truncated projections. Algorithms based on the Radon inversion formula such as the CBP when directly used with truncated projections does not properly reconstruct the object function outside the field of view. In addition, artefacts extend into the field of view [3,4,5]. Thus indirect methods are being devised so that a fairer reconstruction can be obtained from truncated projections.

Iterative methods such as Algebraic Reconstruction Technique (ART) and Simultaneous Iterative Reconstruction Technique (SIRT) have been investigated for reconstruction from truncated projections [6]. A major dis-advantage of this approach is that it requires considerable amount of computer time. Several authors have shown that reasonable accurate images with lesser artefacts could still be obtained from the CBP method of reconstruction using 'completed' truncated projections [3,4,5]. The completion of projection in [3] is achieved by estimating the missing data by fitting polynomial functions to a few end points on either side of the truncated projection. In [5], the cross sectional outline of the object function is obtained by optical methods and the missing projection data is approximated as the product of the path length and a mean value of the object function which is estimated from the available data. This paper presents a method for completing the truncated projection using Linear Prediction theory, thereby enabling algorithms based on Radon inversion formula to extract significantly more information from incomplete projections.

Projection completion by Linear Prediction

Linear predictor models have been developed for many signals for different applications such as prediction or forecasting, control, data compression and spectral estimation. One of the most widely investigated model for extrapolating a truncated signal or interpolating a spectral density function is the Autoregressive (AR) model. Fitting an AR model to the available one dimensional data is equivalent to the Maximum Entropy Method [7]. Maximum entropy processing ensures that fewest possible assumptions are made about the unmeasured data. This is the motivation for modelling the projection data as an output of a linear predictor.

Simulation Results

Let $g(x,y)$ represent a two dimensional object function which is zero outside a circle of radius b (Fig. 1). The Radon transform $[Rg](\theta, t)$ is the line integral of the function along the line AB (Fig.1).

$$[Rg](\theta, t) = \int_{AB} g(x,y) ds$$

where ds is the elemental distance on the line AB represented by the equation $x \cos \theta + y \sin \theta = t$. The projection $[Rg](\theta, t)$ is a set of line integrals evaluated along parallel lines perpendicular to the vector which makes an angle θ with the x -axis as shown in Fig. 1.

Consider a data matrix P where an element $p(i,j)$ represents a line integral $[Rg](i,j)$ and each row represents a complete projection at an angle i . A truncated projection manifests itself as missing columns in the data matrix. Fig. 2 depicts the limited field of view situation where the ROI ($r < a$ in Fig. 1) is projected from all directions $0^\circ \leq \theta < 179^\circ$. Each of the available truncated projection, a row in the data matrix, is modelled as an AR process of order N . $p(i,j)$ is expressed approximately as a linear combination of the 'past' values.

$$\hat{p}(i,j) = - \sum_{k=1}^N a_N(k) p(i,j-k)$$

where $\hat{p}(i,j)$ is an approximation of $p(i,j)$ and $a_N(k)$ are the AR coefficients of order N . The error or residual between the actual value of $p(i,j)$ and the predicted value $\hat{p}(i,j)$ is given by

$$e(j) = p(i,j) - \hat{p}(i,j) = \sum_{k=0}^N a_N(k) p(i,j-k)$$

where $a_N(0) = 1$.

The AR parameters are obtained by minimising the mean or total squared error with respect to each of the parameters. Various algorithms are available to obtain the AR coefficients [8]. Each projection is then completed by extrapolating the truncated projection forwards and backwards using the derived linear predictor. The finite extent of the object which may be known a priori or can be determined experimentally is used to determine the number of points to be extrapolated on either side. If data points in the extrapolated segment are negative, they are set to zero. The completed projection thus consists of the original truncated projection and the extrapolated segments. The completion of the data matrix is thus achieved without making any assumptions such as the object function is zero or constant for the area outside the ROI ($a < r < b$) nor it requires any extra measurements outside the ROI.

The test phantom composed of 9 superimposed ellipses of size (64×64) used in the computer simulation studies is shown in Fig. 3. 180 equispaced projections, each sampled at 91 values of t (corresponding to a parallel projection) distributed uniformly over the full field of view ($a=45$) encompassing the whole phantom were computed. The reconstruction of the phantom was carried out with this full data using the CBP method (Fig. 4). The Ramachandran - Lakshminarayan filter [1] and a Hamming window was used for filtering and smoothing the projection data. This operation was carried out in the frequency domain using FFT algorithms. A weighted backprojection was then used to obtain the reconstructed image. In order to simulate the measurements of truncated projections, the outer parts of the projection data corresponding to rays which do not intersect the circular region of interest ($r > a$) were set to zero. Three cases of the ROI with $a = 35, 30$ and 25 are considered. Fig. 5a, 6a and 7a shows the reconstruction obtained by using the CBP method directly with the truncated projections for the three cases $a=35, a=30$ and $a=25$ respectively. The errors present are evidently considerable. Completion of the truncated projections were then carried out as mentioned in the previous section assuming an elliptical boundary. A study of the partial autocorrelation function and the residual for various projections showed that an AR model of order 5 was sufficient to model the truncated data in the present case. The Burg algorithm [9] which is found to be efficient for short data lengths was used to obtain the AR coefficients directly from the data values. Fig. 5b, 6b and 7b shows the effectiveness of the proposed method of completion of the truncated projections for the three cases respectively. For the sake of comparison, the reconstruction obtained by using the positive constraint additive ART method with truncated projection for the first two cases $a=35$ and $a=30$ are shown in Fig. 8 and 9.

Conclusion

The proposed method of completing the truncated projections results in a significantly better reconstruction compared to the reconstruction obtained by using the incompleted ones. Qualitatively the reconstructed images are very good within the field of view. Also, features which are visually missing in the region outside the field of view can be seen when the truncated projections are completed, although quantitative errors can be observed. A detailed error analysis is being carried out. An advantage of this method is that it does not require additional measurements outside the field of view. The time taken for the completion of the truncated projections is insignificant. The method is being extended to include the other two cases - the hollow and the limited angle situations.

Prediction essentially relies on the fact that the linear predictor is able to extract the correlation present in the data. The simple completion method presented here models each of the projection individually using a one dimensional predictor model. This overlooks the fact that all the projections are not actually independent as they are all derived from the same cross section. In order to exploit this fact, further investigations are being carried out using two dimensional linear predictor models and block adaptive methods.

References

- [1] G.N.Ramachandran and A.V.Lakshminarayan, 'Three dimensional reconstruction from radiographs and electron micrographs : Application of Convolution instead of Fourier Transform', Proc. Nat. Acad. Sci., vol.68, pp2236-2240, 1971.
- [2] A.K.Louis and F.Natterer, 'Mathematical problems of Computerized Tomography', Proc. IEEE, vol.71, pp379-389, 1983.
- [3] R.M.Lewitt and R.H.T.Bates, 'Image reconstruction from projections', Optik, vol. 50, Part I: pp19-33; Part III : pp189-204, 1978.
- [4] J.C.Gore and S.Leeman, 'The reconstruction of objects from incomplete projections', Phys. Med. Biol., Vol.25, pp129-136, 1980.
- [5] W.Wagner, 'Reconstructions from restricted region scan data - New means to reduce the patient dose', IEEE Trans. Nucl. Sci., Vol. NS-26, pp2866-2869, April 1979.
- [6] B.E.Oppenheim, 'More accurate algorithms for iterative 3-dimensional reconstruction', IEEE Trans. Nucl. Sci., NS-21, pp72-77, 1974.
- [7] A.VanDenBos, 'Alternative interpretation of maximum entropy spectral analysis', IEEE Trans. Inform. Theory, Vol.IT-17, pp493-494, 1971.
- [8] V.Krishnan, 'Adaptive Estimation Algorithms', Lecture Notes, Indian Institute of Science, Bangalore, India, October 1984.
- [9] J.P.Burg, 'A new analysis technique for time series data', presented at the NATO Advanced Study Inst. Signal Processing with emphasis on Underwater Acoustics, Enschede, Netherlands, 1968.

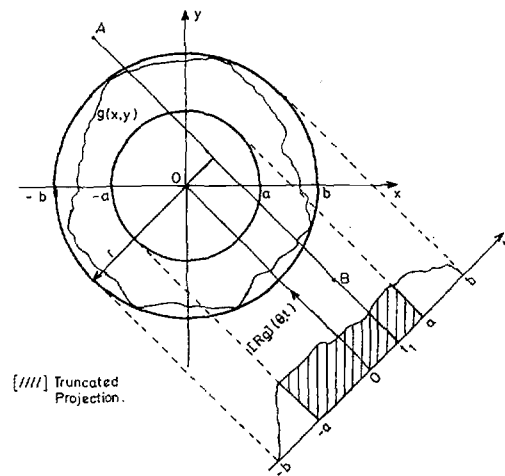


Fig.1. Function $[Rg](\theta_t)$ the projection of $g(x,y)$ at angle θ .

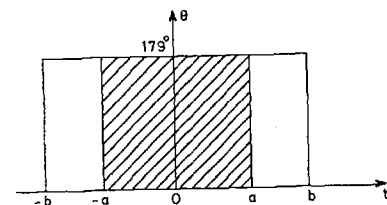


Fig.2. Truncated projections: $[Rg](\theta_t)$ is known only for the lines intersecting the hatched area.

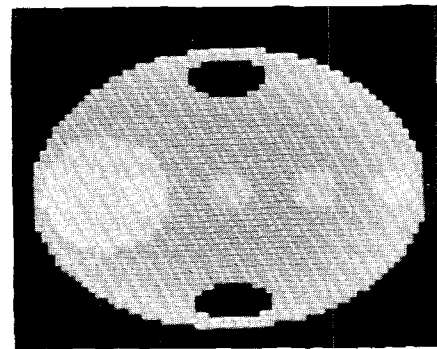


Fig. 3

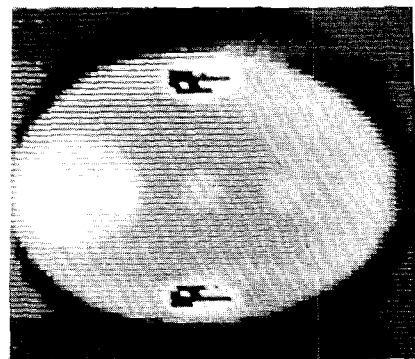


Fig. 4

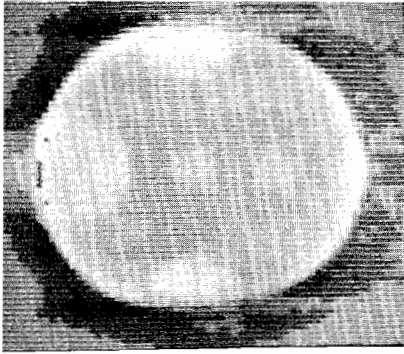


Fig. 5a

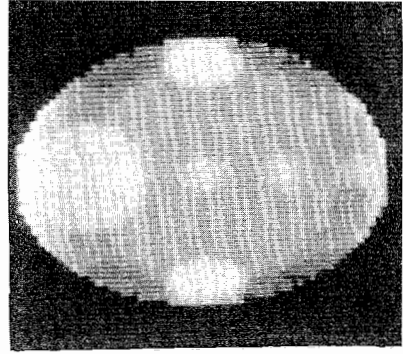


Fig. 5b

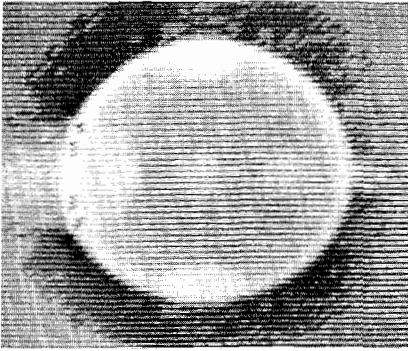


Fig. 6a

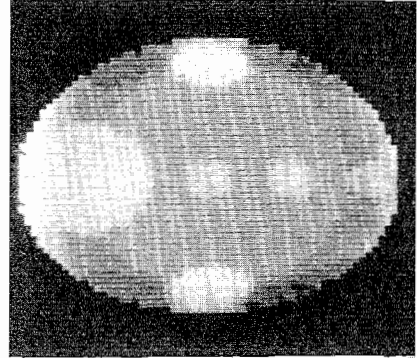


Fig. 6b

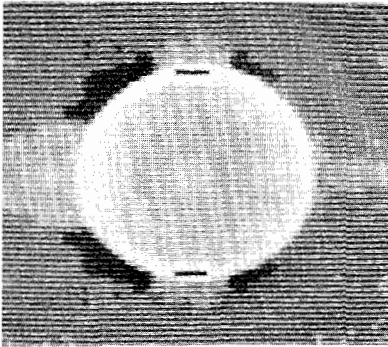


Fig. 7a

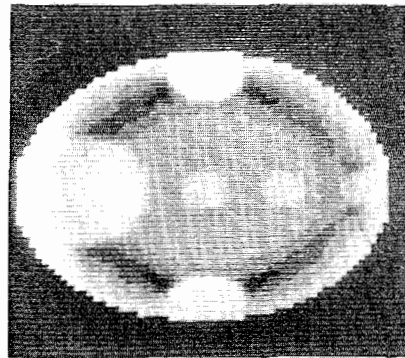


Fig. 7b

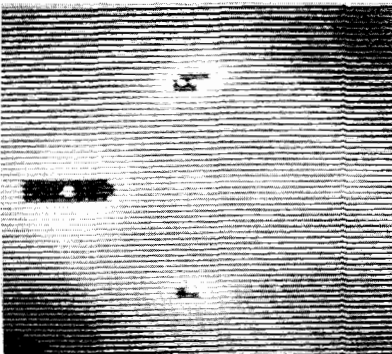


Fig. 8

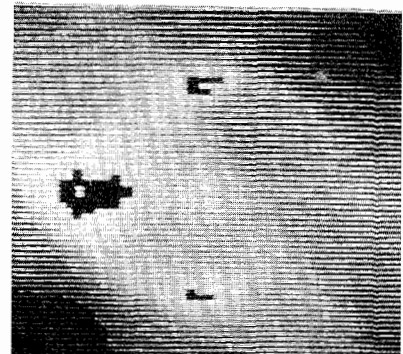


Fig. 9